Effective temperature of ionizing stars of extragalactic H II regions

O. L. Dors[1]⋆, G. F. Hägele[2,3], M. V. Cardaci[2,3], A. C. Krabbe[1]

[1] *Universidade do Vale do Paraíba, Av. Shishima Hifumi, 2911, Cep12244-000, São José dos Campos, SP, Brazil*
[2] *Instituto de Astrofísica de La Plata (CONICET-UNLP), Argentina.*
[3] *Facultad de Ciencias Astronómicas y Geofísicas, Universidad Nacional de La Plata, Paseo del Bosque s/n, 1900 La Plata, Argentina.*

ABSTRACT

The effective temperature ($T_{\rm eff}$) of the radiation field of the ionizing star(s) of a large sample of extragalactic H II regions was estimated using the $R=\log([\text{O II}](\lambda\lambda3726+29)/[\text{O III}]\lambda5007)$ index. We used a grid of photoionization models to calibrate the $T_{\rm eff}$-R relation finding that it has a strong dependence with the ionizing parameter while it shows a weak direct dependence with the metallicity (variations in Z imply variations in U) of both the stellar atmosphere of the ionizing star and the gas phase of the H II region. Since the R index varies slightly with the $T_{\rm eff}$ for values larger than 40 kK, the R index can be used to derive the $T_{\rm eff}$ in the $30 - 40$ kK range. A large fraction of the ionization parameter variation is due to differences in the temperature of the ionizing stars and then the use of the (relatively) low $T_{\rm eff}$ dependent $S2=[\text{S II}](\lambda\lambda6717+31)/\text{H}\alpha$ emission-line ratio to derive the ionization parameter is preferable over others in the literature. We propose linear metallicity dependent relationships between $S2$ and U. $T_{\rm eff}$ and metallicity estimations for a sample of 865 H II regions, whose emission-line intensities were compiled from the literature, do not show any $T_{\rm eff}$-Z correlation. On the other hand it seems to be hints of the presence of an anti-correlation between $T_{\rm eff}$-U. We found that the majority of the studied H II regions ($\sim$ 87%) present $T_{\rm eff}$ values in the range between 37 and 40 kK, with an average value of 38.5($\pm$1) kK. We also studied the variation of $T_{\rm eff}$ as a function of the galactocentric distance for 14 spiral galaxies. Our results are in agreement with the idea of the existence of positive $T_{\rm eff}$ gradients along the disk of spiral galaxies.

Key words: galaxies: general – galaxies: evolution – galaxies: abundances – galaxies: formation– galaxies: ISM

1 INTRODUCTION

The effective temperature of massive stars is an important parameter to understand the evolution of these objects and their influence on the interstellar medium as well as on the galaxy in which they reside.

In general, the effective temperature of ionizing stars of an H II region (hereafter $T_{\rm eff}$) located in the Milk Way and in the Magellanic Clouds can be estimated through their spectral classifications (see e.g. Evans et al. 2015; Lamb et al. 2015; Walborn et al. 2014; Morrell et al. 2014; Sota et al. 2014, 2011; Massey et al. 2009, 2005; Conti et al. 2007). However, for more distant stars, the $T_{\rm eff}$ can be only estimated indirectly, i.e. through the analysis of the

emission-lines emitted by the nebulae ionized by these stars. The original idea was proposed by Zanstra (1931) and consist in assuming that, if the nebula around of a star is optically thick to the Lyman continuum, it absorbs all the ionizing photons emitted by the star. Thus, the number of ionizations per unit of time in the nebula or the flux of a given emission-line is directly proportional to the number of ionizing photons emitted by the star as well as dependent on its effective temperature (Osterbrock 1989). Along decades, this method have been improved by several authors, mainly in the sense of defining what nebular lines can be used to constrain $T_{\rm eff}$ in Planetary Nebulae and in H II regions (e.g. Ambarzumian 1932; Stoy 1933; Gurzadyan 1955; Kaler 1976; Chopinet & Lortet-Zuckermann 1976; Kaler 1978; Koppen & Tarafda 1978; Iijima 1981; Mathis 1985; Stasińska & Tylenda 1986; Vílchez & Pagel

⋆ E-mail: olidors@univap.br

1988; Bresolin et al. 1999; Kennicutt et al. 2000; Oey et al. 2000; Dors & Copetti 2003; Morisset 2004; Pérez-Montero & Vílchez 2009; Zastrow et al. 2013).

T_{eff} determinations for the majority of extragalactic H II regions are obtained comparing observed emission-line fluxes with those predicted by nebular photoionization models assuming as ionizing source a star with a given temperature (e.g. Zastrow et al. 2013; Pellegrini, Baldwin, & Ferland 2011; Morisset 2004; Dors & Copetti 2003; Kennicutt et al. 2000; Vílchez & Pagel 1988). However, nebular emission-lines depend primarily on three parameters: T_{eff}, metallicity and ionization parameter (Oey et al. 2000). Thus, it is necessary produce estimations of two of these parameters to derive the third. Kennicutt et al. (2000), who used optical data of H II regions located in the Milk Way and the Magellanic Clouds, compared T_{eff} estimations based on emission-lines predicted by photoionization models with values obtained from stellar spectral classifications. These authors observed a strong degeneracy between forbidden-line sequences produced by changes in T_{eff} and metallicity of the gas phase of the nebulae, which shows the difficulty of using emission-line ratios as T_{eff} indicators.

Likewise, Morisset (2004), who compared diagnostic diagrams containing observational infrared emission-lines of Galactic H II regions and predictions from photoionization models, showed that if the metallicity and the ionization parameter of the gas phase of the nebulae are not taking into account, erroneous T_{eff} values can be obtained. Moreover, Pellegrini, Baldwin, & Ferland (2011) showed that T_{eff} can be determined through sets of diagnostic diagrams containing photoionization model predictions of emission lines dependent on the radiation flux emitted by the ionizing source and on the ionizing parameter, but weakly dependent on the metallicity and the electron density of the gas. This methodology permits to break the degeneracy in T_{eff} estimations. Most recently, Zastrow et al. (2013) compared long slit observations of a sample of H II regions located in the Large Magellanic Cloud with predictions of photoionization models in order to estimate the T_{eff} of these objects. These authors pointed out the need in estimating the metallicity and the ionizing parameter before using the models to calculate the T_{eff}.

To eliminate the degeneracy in the T_{eff} estimations it is required to calculate the metallicity (Z) of the gas phase (generally traced by the relative abundances between oxygen and hydrogen, O/H) and the ionization parameter of the H II regions considered. Concerning the first parameter, accurate metallicities of H II regions can only be derived by measuring auroral emission-lines (e.g. [O III]$\lambda4363$) which are very weak or unobservable in H II regions with high metallicity and/or low excitation (Bresolin et al. 2005; Díaz et al. 2007). Therefore, for most of the cases, the method based on calibration between strong emission-lines and oxygen abundances proposed by Pagel et al. (1979) are used to estimate Z (see also Pilyugin et al. 2012; Peña-Guerrero et al. 2012; Dors & Copetti 2005; Kennicutt et al. 2003; Kewley & Dopita 2002; Pilyugin 2001). Concerning the ionizing parameter U, Díaz et al. (1991) and Dors et al. (2011) derived calibrations between emission-line ratios easily measurable and U, which can be used to eliminate the degeneracy in the T_{eff} estimations.

Nowadays, despite the large amount of spectroscopic data of H II regions available in the literature, such as the data produced by the CALIFA survey (Sánchez et al. 2012), T_{eff} has been estimated for few extragalactic objects. In fact, Kennicutt et al. (2000) estimated the T_{eff} for 39 H II regions, being only 10 objects located in the Magellanic Clouds. Dors & Copetti (2003), using the line ratio $R = \log([\text{O II}](\lambda\lambda3726+29)/[\text{O III}]\lambda5007)$ and the spectroscopic data of Kennicutt & Garnett (1996), derived T_{eff} values for exciting stars located in the disk of the spiral galaxy M 101 (see also Evans 1986; Vílchez & Pagel 1988; Henry & Howard 1995; Zastrow et al. 2013).

In this paper we also used the $R = \log([\text{O II}](\lambda\lambda3726+29)/[\text{O III}]\lambda5007)$ index to estimate the T_{eff} for a large sample of extragalactic H II regions. Our study is motivated by the following goals:

(i) To produce a calibration between R and T_{eff} taking into account the effects of the ionizing parameter and the metallicity of both nebular gas and stellar atmosphere of the ionizing star on this relation.

(ii) To estimate T_{eff} values for a large sample of extragalactic H II regions and investigate the dependence of T_{eff} with the metallicity and with the ionization parameter.

(iii) To investigate the variation of T_{eff} with the galactocentric distance in spiral galaxies in order to verify if gradients of this parameter are an universal property of these objects.

The photoionization models used to obtain an R-T_{eff} calibration are described in Sect. 2. The data sample used to derive T_{eff} values are presented in Sect. 3. The methodology employed and the sources of uncertainties are described in Sects. 4 and 5, respectively. In Sect. 6 and 7 the results and discussion of the outcome are presented. The final conclusions are given in Sect. 8.

2   PHOTOIONIZATION MODELS

We employed the CLOUDY code version 13.00 (Ferland et al. 2013) to build a grid of photoionization models in order to derive calibrations among the parameters T_{eff} and U and strong nebular emission-lines, easily measurable in observations of H II regions. In what follows the main parameters of the models are described.

• Metallicity – The metallicity Z of the gas phase of the hypothetical nebulae was linearly scaled with the solar metallicity $Z_\odot$, considering the solar oxygen abundance $12 + \log(\text{O/H})_\odot = 8.69$ (Allende-Prieto et al. 2001). The nitrogen abundance was taken from the relation $\log(\text{N/O}) = \log(0.034 + 120\,\text{O/H})$ of Vila Costas & Edmunds (1993). We considered the values Z=1.0, 0.5, 0.2 and 0.03 $Z_\odot$. The presence of internal dust was considered and the grain abundances (van Hoof et al. 2001) were also linearly scaled with Z. Depletion of refractory elements onto dust grains was considered as in Dors & Copetti (2005).

• Electron density – We considered the electron density as being $100\ \text{cm}^{-3}$. This value is in the range of values derived for extragalactic H II regions (Sanders et al. 2016; Krabbe et al. 2014; Copetti et al. 2000).

• Stellar atmosphere model – We use the public stellar atmosphere models WM-basic (Pauldrach et al. 2001) that are already available in the stellar atmosphere library in the CLOUDY code (Ferland et al. 2013). We considered the WM-basic models because, among the stellar atmosphere

models assumed in the photoionization model grids built by Zastrow et al. (2013), they produced the best agreement between predicted and observed optical emission-line ratios. The $T_{\rm eff}$ values ranged from 30 000 to 50 000 K, with a step of 2500 K, where the metallicity (Z) of the stellar atmosphere was considered to be the same than the one of the nebular gas. This $T_{\rm eff}$ range is the same that the one considered by Morisset (2004).

The value of the solar metallicity is a current question of debate (see Caffau et al. 2016) and it is constantly updated in the CLOUDY code[1], which can yield an incorrect match between the abundances of some particular element in the gas phase of the nebulae and in the stellar atmosphere. Unfortunately, this problem can not be resolved because the assumed abundance values for the majority of the elements in stellar atmosphere models are, many times, not declared and only a general value of the metallicity is given.

• Ionization parameter – It is defined as $U = Q_{\rm ion}/4\pi R_{\rm in}^2 nc$, where $Q_{\rm ion}$ is the number of hydrogen ionizing photons emitted per second by the ionizing source, $R_{\rm in}$ is the distance from the ionization source to the inner surface of the ionized gas cloud (in cm), n is the particle density (in cm^{-3}), and c is the speed of light. We considered $\log U$ ranges from -3.5 to -1.5 dex, with a step of 0.5 dex. The variation in the value of U simulates the excitation differences of H II regions, mass, or geometrical conditions in a wide range of possible scenarios (Pérez-Montero 2014). It is worth mentioning that models with different combination of $Q_{\rm ion}$, R and n but that result in the same U are homologous models with the same predicted emission-line intensities (Bresolin et al. 1999).

In total, 180 photoionization models were built. The $T_{\rm eff}$ value estimated through the R index should be interpreted as the temperature of the hottest star of the ionizing stellar cluster of the H II region, since this star drives the emission of the ionizing photons (Zastrow et al. 2013).

3   DATA SAMPLE

Observational emission-line intensities of a sample of extragalactic H II regions were compiled from the literature. We considered only H II regions for which the intensities, relative to Hβ, of the [O II]$\lambda\lambda3726+29$, [O III]$\lambda5007$, Hα, and [N II]$\lambda6584$, and [S II]$\lambda\lambda6717+31$ emission-lines were measured. All emission line intensities are reddening corrected. For some few cases in which the Hα intensity is not presented, we calculated it from the theoretical ratio Hα/H$\beta = 2.86$ (Hummer & Storey 1997). Indeed, when only the sum of [O III]($\lambda4959+\lambda5007$) and/or [N II]($\lambda6548+\lambda6584$) are listed in the original papers from which the data were compiled, the intensities of [O III]$\lambda5007$ and [N II]$\lambda6584$ were calculated assuming the theoretical relations [O III]$\lambda5007 \approx 3.0 \times$ [O III]$\lambda4959$ and [N II]$\lambda6584 \approx 3.00 \times$ [N II]$\lambda6548$ (Storey & Zeippen 2000), respectively.

To exclude objects with a secondary ionizing source, we use the criterion proposed by Kewley et al. (2001) to separate objects ionized by massive stars from those containing
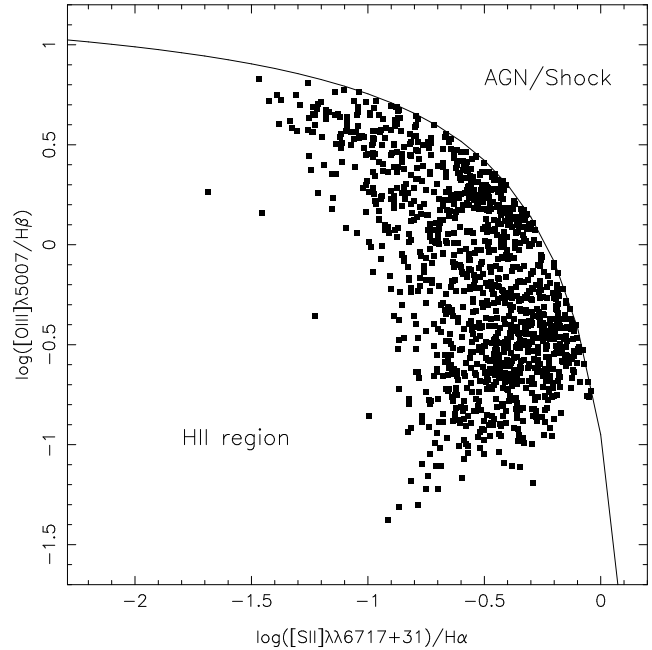

Figure 1. $\log([\text{O III}]\lambda5007/\text{H}\beta)$ vs. $\log([\text{S II}](\lambda\lambda6717+31)/\text{H}\alpha)$ diagnostic diagram. The solid line represents the relation by Kewley et al. 2001. It separates objects ionized by massive stars from those containing active nuclei and/or shock-excited gas, as indicated. Squares represent the observational data (see Sect. 3).

gas shock and/or active galactic nuclei (AGN), where all objects with

$$\log([\text{OIII}]\lambda5007/\text{H}\beta) > \frac{0.72}{\log([\text{S II}](\lambda\lambda6717+31)/\text{H}\alpha) - 0.32} + 1.30 \quad (1)$$

were not considered in our sample. We selected 1198 extragalactic H II regions located in 44 galaxies with redshift $z < 0.5$.[2] In Table 1 we listed the bibliographic references of the sample, the host galaxy of the H II regions and the number of objects taken from each work. In Fig. 1, a diagnostic diagram $\log([\text{O III}]\lambda5007/\text{H}\beta)$ versus $\log([\text{S II}]\lambda\lambda6717+31+/\text{H}\beta)$ proposed by Veilleux & Osterbrock (1987), the observational data and the relation by Kewley et al. (2001) are shown.

4   METHODOLOGY

4.1 $T_{\rm eff}$ estimation

To estimate the $T_{\rm eff}$ value of a given H II region, we adopted a similar methodology to the one presented by Dors & Copetti (2003), in which photoionization model results were considered to derive a relation between $T_{\rm eff}$ and the $R = \log([\text{O II}](\lambda\lambda3726+29)/[\text{O III}]\lambda5007)$ index. However, Dors & Copetti (2003) did not present an expression to derive $T_{\rm eff}$ since they only considered models with $Z_\odot$ and with a fixed ionization parameter value ($< \log U >= -2.5$). In this work, the Z and U parameters are taking into account in $T_{\rm eff}$ estimations.

In Fig. 2, the relations between $T_{\rm eff}$ and R for different Z

---

[1] see also *http : //www.nublado.org/wiki/RevisionHistory*

Table 1. The sample.

Reference	Galaxy	Number of H II regions
Kennicutt et al. (2000)	Magellanic Clouds	8
Vermeij et al. (2002)	Magellanic Clouds	6
Russel & Dopita (1990)	Magellanic Clouds	5
Zurita & Bresolin (2012)	M 31	12
Garnett et al. (1997)	NGC 2403	8
Van Zee et al. (2000)	UGCA 292	2
Bresolin et al. (2004)	M 51	10
Kennicutt et al. (2003)	M 101	25
Vílchez et al. (1988)	M 33	5
Kwitter & Aller (1981)	M 33	10
López-Hernández et al. (2013)	M 33	9
Bresolin et al. (2009a)	NGC 300	16
Lee & Skillman (2004)	NGC 1705	13
López-Sánchez & Esteban (2009)	Mkn 1199	5
López-Sánchez & Esteban (2009)	Mkn 5	2
López-Sánchez & Esteban (2009)	IRAS 08208+2816	4
López-Sánchez & Esteban (2009)	III Zw107	3
López-Sánchez & Esteban (2009)	Tol 1457-262	1
López-Sánchez et al. (2011)	IC 10	7
López-Sánchez et al. (2007)	NGC 5253	4
Esteban & Méndez (1999)	Mkn 8	5
Berg et al. (2013)	NGC 628	13
Bresolin et al. (2009b)	M 83	24
Bresolin et al. (2012)	NGC 1512	50
Bresolin et al. (2012)	NGC 3621	71
Van Zee et al. (1998)	NGC 925	24
Van Zee et al. (1998)	NGC 1068	1
Van Zee et al. (1998)	NGC 1232	16
Van Zee et al. (1998)	NGC 1637	16
Van Zee et al. (1998)	NGC 2805	17
Van Zee et al. (1998)	IC 2458	3
Van Zee et al. (1998)	NGC 2820	4
Van Zee et al. (1998)	NGC 2903	9
Van Zee et al. (1998)	NGC 3184	17
Van Zee et al. (1998)	NGC 4395	9
Hägele et al. (2012)	Haro 15	2
Hägele et al. (2011)	SDSS J165712.75+321141.4	3
Díaz et al. (2007)	NGC2903	4
Sánchez et al. (2012)	UGC 9837	64
Sánchez et al. (2012)	NGC 1058	258
Sánchez et al. (2012)	UGC 9965	56
Sánchez et al. (2012)	NGC 1637	148
Sánchez et al. (2012)	NGC 3184	58
Sánchez et al. (2012)	NGC 3310	103
Sánchez et al. (2012)	NGC 4625	42
Sánchez et al. (2012)	NGC 5474	79
Sánchez et al. (2012)	NGC 628	165

and U values are shown. As can be seen, the $T_{\rm eff}$-R relation presents two behaviours for the ranges of values $T_{\rm eff}$= 30-40 and 40-50 (10^3 K). Therefore, we considered different linear regressions for these ranges whose coefficients are listed in Table 2. In Fig. 2 we can note the strong dependence of the $T_{\rm eff}$-R relation with the ionization parameter. In opposite, the metallicity has a secondary influence on this relation. Moreover, we can see that the R index presents little variations for $T_{\rm eff} > 40$ kK, result also found by Oey et al. (2000) and Kennicutt et al. (2000) for other line-ratios. Hence, for temperatures higher than 40 kK, small emission-line variations or measurement errors translate into very large un-

certainties in the $T_{\rm eff}$ estimations. Thus, despite the $T_{\rm eff}$-R fitting results are presented in Table 2, along this paper, we only consider $T_{\rm eff}$ values $\leqq$ 40 kK. The relations derived for the highest temperatures could be used only to estimate the order of magnitude of the radiation field effective temperature.

4.2 Z estimations

To estimate the metallicity Z, we use strong-line methods. Nowadays, several authors have proposed empirical calibrations of Z with different strong emission lines combinations
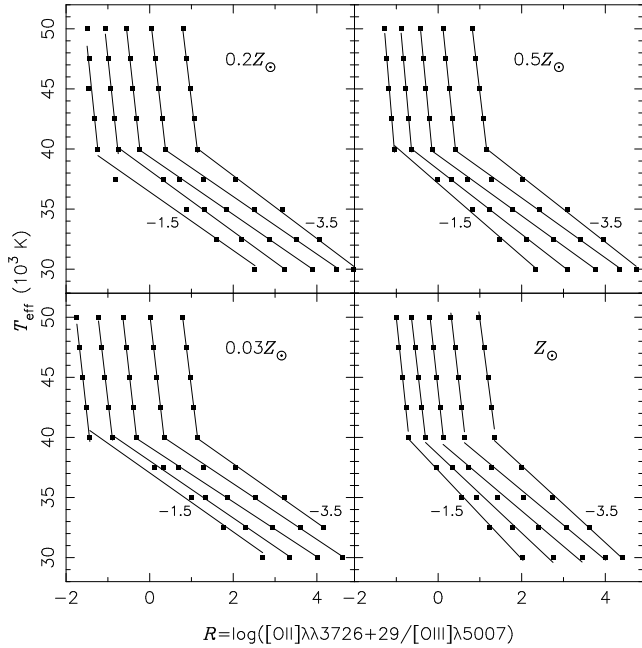
Figure 2. $T_{\rm eff}$ vs. R assuming different values for the metallicity Z and the ionizing parameters U as indicated. Points represent results of the photoionization models (see Sect. 2). Lines represent the linear regression fittings whose coefficients are listed in Table 2.

(see López-Sánchez & Esteban 2009 for a review) and different calibrations can produce values in disagreement from each other by until 0.7 dex (Kewley & Ellison 2008).

However, since there is consensus that the $T_{\rm e}$-method yields more reliable metallicity (or abundance) estimations, empirical calibrations based on direct determinations of the electron temperature of nebulae (Pilyugin 2001, 2000) are preferable than those relations theoretically developed (see, for example, the calibrations proposed by Kewley & Dopita 2002). Moreover, this kind of strong emission-line calibrations have an advantage with respect to the others since the physical conditions of the nebulae (established by $T_{\rm eff}$, geometry, mass, etc, essential ingredients in order to estimate the abundance) are taken into account via the direct determination of the electron temperature.

Therefore, along this paper, we used a strong emission-line calibration to estimate the metallicities. In particular we adopted the empirical calibration proposed by Pilyugin & Grebel (2016)

$$\begin{aligned} 12 + {\rm (O/H)}_{R,2D} &= 8.589 + 0.329 \log N_2 + \\ &+ (-0.205 + 0.549 \log N_2) \times \log R_2, \end{aligned} \quad (2)$$

where $N_2 = I_{\rm [N\,II]\lambda\lambda6548+84}/I_{\rm H\beta}$ and $R_2 = I_{\rm [O\,II]\lambda\lambda3726+29}/I_{\rm H\beta}$.

4.3 U estimations

Concerning calibrations between U and strong emission-lines, Díaz et al. (1991), Dors et al. (2011), Sanders et al. (2016) and Morisset et al. (2016), using photoionization model results, proposed theoretical relations between this parameter and [S II]($\lambda\lambda6717+31$)/[S III]($\lambda\lambda9069+9532$), [O II]$\lambda\lambda3726+29$/[O III]$\lambda5007$ and [S II]($\lambda\lambda6717 + 31$)/Hα)

Table 2. Coefficients of the linear regression $T_{\rm eff} = {\rm a} \times R + {\rm b}$ estimated for two different ranges of $T_{\rm eff}$ (in units of 10^3 K), where $R = \log({\rm [O\,II]}\lambda\lambda3726+29/{\rm [O\,III]}\lambda5007)$.

	$T_{\rm eff} = 30-40$		$T_{\rm eff} = 40-50$	
$\log U$	a	b	a	b
$Z = Z_\odot$				
-1.5	-3.69 ± 0.10	37.27 ± 0.12	-33.17 ± 2.39	16.85 ± 2.05
-2.0	-3.27 ± 0.20	38.60 ± 0.31	-30.00 ± 0.60	30.88 ± 0.29
-2.5	-2.95 ± 0.20	39.78 ± 0.41	-31.54 ± 0.84	43.95 ± 0.09
-3.0	-2.90 ± 0.14	41.39 ± 0.37	-30.43 ± 1.71	59.65 ± 0.85
-3.5	-3.20 ± 0.10	44.05 ± 0.31	-26.36 ± 2.15	76.17 ± 2.56
$Z = 0.5\,Z_\odot$				
-1.5	-3.02 ± 0.13	37.14 ± 0.17	-42.48 ± 2.24	-4.58 ± 2.63
-2.0	-2.70 ± 0.02	38.30 ± 0.05	-38.98 ± 1.76	15.12 ± 1.36
-2.5	-2.52 ± 0.04	39.48 ± 0.09	-36.84 ± 1.01	34.47 ± 0.30
-3.0	-2.50 ± 0.05	40.93 ± 0.16	-33.52 ± 0.54	53.94 ± 0.15
-3.5	-2.73 ± 0.08	43.18 ± 0.26	-29.43 ± 0.28	74.10 ± 0.28
$Z = 0.2\,Z_\odot$				
-1.5	-2.44 ± 0.24	36.44 ± 0.37	-33.36 ± 7.28	-1.39 ± 10.16
-2.0	-2.54 ± 0.04	38.21 ± 0.08	-32.14 ± 2.81	15.47 ± 2.60
-2.5	-2.40 ± 0.03	39.35 ± 0.07	-31.63 ± 0.99	32.52 ± 0.40
-3.0	-2.39 ± 0.05	40.82 ± 0.15	-30.50 ± 0.40	51.47 ± 0.09
-3.5	-2.62 ± 0.07	43.04 ± 0.26	-28.69 ± 0.23	72.69 ± 0.23
$Z = 0.03\,Z_\odot$				
-1.5	-2.46 ± 0.20	37.06 ± 0.33	-31.45 ± 2.04	-5.31 ± 3.28
-2.0	-2.38 ± 0.05	38.06 ± 0.11	-29.67 ± 1.10	13.42 ± 1.18
-2.5	-2.28 ± 0.02	39.20 ± 0.06	-30.58 ± 0.59	30.37 ± 0.29
-3.0	-2.30 ± 0.05	40.70 ± 0.15	-30.01 ± 0.26	50.33 ± 0.05
-3.5	-2.45 ± 0.08	42.72 ± 0.23	-28.08 ± 0.23	72.16 ± 0.23

emission-line ratios. A large fraction of the variation of U is due to differences in the temperature of the ionizing stars through the amount of the hydrogen ionizing photons.

Among the line ratios above, we consider a calibration between the ionization parameter U and the emission-lines ratio defined as

$$S2 = \log({\rm [S\,II]}(\lambda\lambda6717 + 31)/{\rm H}\alpha). \quad (3)$$

This emission-line ratio is preferable to be used to derive U due to its (relatively) low dependence on the $T_{\rm eff}$. In fact, Pellegrini, Baldwin, & Ferland (2011) used diagnostic diagrams containing several model-predicted and observed emission-line ratios in order to study the physical conditions and ionization mechanisms across the 30 Doradus H II region. By using a large grid of models built with the CLOUDY code (Ferland et al. 2013), these authors showed that, for a fixed metallicity value, $S2$ has a maximum variation of ~ 0.2 dex for models with $T_{\rm eff}$ ranging from 36 kK to 44 kK. (see Fig.5(b) of Pellegrini, Baldwin, & Ferland 2011).

In Fig. 3, the results of our models for the relation $\log U$-$S2$ and for different metallicity and $T_{\rm eff}$ values are shown. Results for $T_{\rm eff}$ values of 30 kK and 50 kK are linked by solid lines. We can see that, for $(Z/Z_\odot) \geqq 0.2$ and for a fixed value of $S2$, $\log U$ ranges up to ~ 0.2 dex when $T_{\rm eff}$ varies between 30 kK and 50 kK. A higher variation, up to ~ 0.4 dex, is obtained for $(Z/Z_\odot) < 0.2$.

In order to produce an expression for the $\log U$-$S2$ re-

Table 3. Coefficients of the fitting $\log U = a \times S2 + b$, calculated for different ranges of $Z/Z_\odot$ and from the average of $S2$ values for each $\log U$, where $S2 = \log[\text{S II}](\lambda\lambda 6717 + 31)/\text{H}\alpha$.

$Z/Z_\odot$	a	b
0.03	$-1.57(\pm 0.11)$	$-5.26(\pm 0.20)$
0.20	$-1.56(\pm 0.08)$	$-4.11(\pm 0.09)$
0.50	$-1.68(\pm 0.05)$	$-3.79(\pm 0.04)$
1.00	$-1.80(\pm 0.05)$	$-3.81(\pm 0.04)$
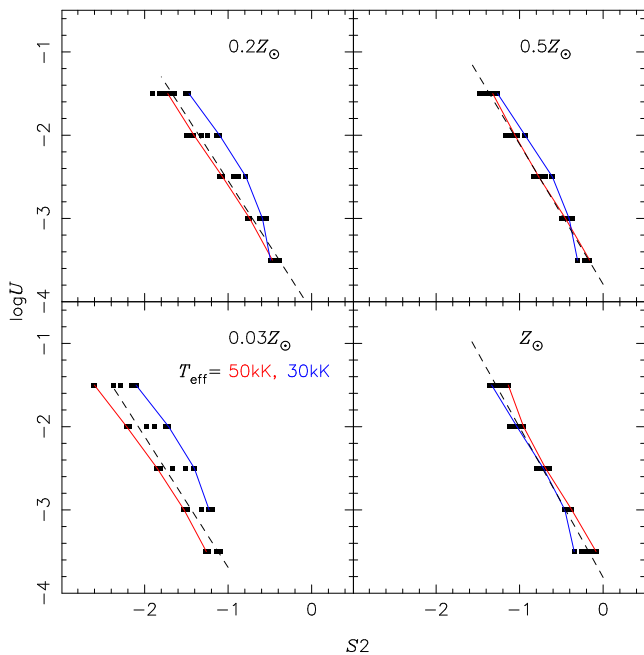
Figure 3. Logarithm of the ionization parameter ($\log U$) versus the line ratio $S2 = \log[\text{S II}](\lambda\lambda 6717 + 31)/\text{H}\alpha$ for different values of metallicity ($Z/Z_\odot$) and different T_{eff} values, as indicated. Points, linked by solid lines, represent the results of our photoionization models (see Sect. 2) for T_{eff} values of 30 kK and 50 kK, as indicated. Dashed lines represent linear regression on the average of $S2$ values for each $\log U$, whose the coefficients are listed in Table 3.

lationship that be independent of T_{eff}, we calculated an $S2$ average value for each $\log U$ and did a linear regression for each of the four metallicity values considered. These fitting are represented in Fig. 3 by dashed lines and the coefficients resulting are listed in Table 3. It can be seen that there is a dependence of the coefficients "a" and "b" with the metallicity. Taken into account this dependence we were able to re-write the $\log U$-$S2$ relationship as:

$$\log U = a(Z/Z_\odot) \times S2 + b(Z/Z_\odot), \tag{4}$$

where

$$a = -0.26(\pm 0.04) \times (Z/Z_\odot) - 1.54(\pm 0.02) \tag{5}$$

and

$$b = -3.69(\pm 1.79) \times (Z/Z_\odot)^2 + 5.11(\pm 1.96) \times (Z/Z_\odot) + -5.26(\pm 0.36). \tag{6}$$

A similar expression, taking into account the metallicity dependence on the $\log U$-$S2$, was obtained by Díaz et al. (1991).

5   UNCERTAINTY IN T_{EFF} ESTIMATIONS

The uncertainty in deriving the T_{eff} through emission-lines is mainly due to the error in their measurements and the dependence of these lines with some nebular parameters (e.g. electron density, metallicity, ionization degree, etc.), the presence of multiple ionizing stars within the H II region and/or the fact that the nebular emission could arise from a complex of H II regions rather than a single region. In what follows, each source of uncertainty is analysed.

5.1   Nebular parameters and line-measure uncertainties

5.1.1   Metallicity

Abundance determinations of H II regions have showed that these objects exhibit a large range of metallicity, from $Z \approx Z_\odot$ for the most metallic objects (e.g. Dors et al. 2008; Bresolin et al. 2004; Kennicutt et al. 2003) to $Z \approx Z_\odot/30$ for the poorest ones (e.g. Garnett & Kennicutt 1994; Skillman & Kennicutt 1993). The metallicity is one of the key parameters that control the emission-line intensities and, hence, the relative intensity between the lines. Nevertheless, from Fig. 2 we can see that the relation T_{eff}-R has a weak dependence with the metallicity since the parameter space occupied by the photoionization models with different Z is almost the same. For example, if we assume $R=1$ and $\log U = -2.5$, T_{eff} varies of only ~ 100 K for Z values from 0.03 to 1 $Z_\odot$. However, as shown in Fig. 2, the T_{eff}-R relation is strongly dependent on U which is derived from $S2$, which in turn has a dependence on the metallicity. In fact, if we assume a fixed value for $S2 = -1$ and a metallicity uncertainty of 0.1 dex (Pilyugin & Grebel 2016), by using Eqs. 4-6, we found variations in $\log U$ of ~ 0.25 dex, which translates into a T_{eff} uncertainty of ~ 1.0 kK.

5.1.2   Ionization parameter

Among all nebular parameters, the ionization parameter U is the one has the main influence on the R-T_{eff} relation. In fact, Oey et al. (2000) presented a detailed comparison of spectra of spatially resolved H II regions with photoionization model results. These authors showed that emission lines of species of ions with low ionization degree, such as the $[\text{S II}](\lambda\lambda 6717 + 31)$, have a scatter of about 0.3 dex along the objects analysed, indicating a local variation in the ionization parameter U. Moreover, Pellegrini, Baldwin, & Ferland (2011), who produce a detailed comparison between model predicted and observed emission line intensities of 30 Doradus, showed that variations in U of until 1 dex can be found along this object. Assuming this value, we would have an uncertainty in U of about 0.5 dex. Taking into account this error in U and assuming $R = 1.0$ and $Z/Z_\odot = 1.0$, a T_{eff} error of ~ 2.0 kK was estimated from Fig. 2.

Pellegrini, Baldwin, & Ferland (2011) also showed the influence of the optical depth on the $S2$ ratio, where optically thick models are needed to describe low $S2$ values found in some parts of 30 Doradus. Moreover, these authors also pointed out that many lower metallicity nebular regions in 30 Doradus have $S2$ affected by density, non radiation

bound. Obviously, these process affects the use of $S2$ as a tracer of U.

However, it is worth noting that the values of the ionization parameter based on our U-$S2$ calibration (Eq. 4) must be interpreted as a global nebular parameter since it is derived from observations and models of the integrated flux of the objecs, and this equation can not be used for spatially resolved studies as the one done by Pellegrini, Baldwin, & Ferland (2011) and Oey et al. (2000). In any case, assuming that U is correct by 0.2 dex (see Sect. 4.3), $R = 1.0$ and $Z/Z_\odot = 1.0$, from Fig. 2, we found a $T_{\rm eff}$ uncertainty of ~ 1.0 kK.

5.1.3 Emission line errors

Regarding the uncertainty in the emission-line flux measurements, typical errors for the strong emission-lines involved in our relations are between about 1 and 5% (e.g. Hägele et al. 2008, 2006; Kennicutt et al. 2003). Assuming that the estimation of the $N2$, $R2$ and $S2$ line ratios have errors as high as 6%, it yields an error in Z of $\sim$3% and in U of $\sim$0.1 dex. Taking into account this U uncertainty and also considering an error of 6% for the R index, we found a $T_{\rm eff}$ error of about ~ 0.5 kK due to errors in the emission line measurements.

5.2 Multiple stars presence

It is known that giant star-forming regions are ionized by multiple stars, i.e. by an ionizing cluster containing stars with a large range of mass and evolutive stages (e.g. Pellegrini, Baldwin, & Ferland 2010; Bosch et al. 2001; Mayya & Prabhu 1996). Thus, the derivation of an unique $T_{\rm eff}$ values for these cases could be somewhat uncertain.

To test the effect of the presence of multiple stars in our $T_{\rm eff}$ estimations, we performed a simple analysis. Firstly, we calculated a photoionization model with solar metallicity and ionized by a single star with spectral type O7V. Assuming the calibrations presented by Massey (2011) and de Koter et al. (1997), this star has a mass of about $M=30\ M_\odot$, $T_{\rm eff}=37$ kK and luminosity $\log(L/L_\odot) = 6$. This model predicts the line ratios $(R, N2, R2, S2)=(1.31, 0.93, 1.77, -0.27)$, for which, using the methodology presented in Section 4, we derived $T_{\rm eff} \approx 37.65$ kK.

Secondly, we assumed a photoionization model with the same parameters than the previous one, but having as the ionizing source a stellar cluster, whose spectral energy distribution was obtained from the STARBURST99 synthesis code (Leitherer et al. 1999). We built a synthetic spectrum considering an instantaneous-burst stellar cluster, a Salpeter initial mass function (Salpeter 1955) with an upper mass limit of $M=30\ M_\odot$, an age of 2.5 Myr, a solar metallicity, and the same atmosphere models than the ones used in the models presented in Section 2. According to Leitherer et al. (1999), this stellar cluster has a luminosity of $\log(L/L_\odot) = 8.72$. We found that this model predicts $(R, N2, R2, S2)=(1.52, 0.37, 1.74, -0.80)$, which also indicates $T_{\rm eff} \approx 35.65$ kK.

Thus, we showed that, for giant H II regions generally ionized by a stellar cluster, the assumption of a single star as the main ionizing source of the gas is correct. Therefore, we assume an uncertainty of 2 kK in $T_{\rm eff}$ estimations due to multiple stars presence.

5.3 H II region complex

In general, for distant objects, the observed spectra comprise the flux of a complex of H II regions and the physical properties derived represent an averaged value (e.g. Rosa et al. 2014; Krabbe et al. 2014; Hägele et al. 2013, 2010, 2009, 2007). In principle, this is not critical in our $T_{\rm eff}$ estimations because H II regions comprising the complexes were probably formed from a same parent molecular cloud with similar initial conditions and resulting in similar stellar contents and nebular parameters (see e.g. Kennicutt et al. 2003).

To simulate the $T_{\rm eff}$ estimations in an H II region complex, we use as prototype system two pairs of near H II regions located in the spiral galaxy NGC 2403 and observed by Garnett et al. (1997). These are the pairs VS35-VS24 (refereed as C1) and VS49-VS48 (refereed as C2) located at about 1 kpc and 5.6 kpc from the NGC 2403 centre, respectively. Initially, considering the observational data obtained by Garnett et al. (1997), we derived one $T_{\rm eff}$ value for each individual H II region of each pair. VS35 and VS24 have the emission-line intensity ratios (R, $N2$, $R2$, $S2$) equal to (0.25, 0.45, 2.46, -0.32) and (0.28, 0.43, 2.41, -0.46), that following the methodology presented in Sect. 4, translate into the $T_{\rm eff}$ values of 37.6 kK and 37.5 kK, respectively. Now, adding the emission line fluxes of individual objects VS35 and VS24 we found for C1 $T_{\rm eff} = 37.5$. The same procedure was considered for the VS49 and VS48 and we found about the same $T_{\rm eff}$ values for these individual objects and for C2, i.e. 40 kK. Thus, we show that our method produces an averaged $T_{\rm eff}$ values in H II region complexes and no uncertainties is yielded for distant objects.

Along the paper, we will consider that the $T_{\rm eff}$ estimation is correct by 2.5 kK, the quadratic sum of the uncertainties discussed above.

6 RESULTS

In Fig. 4, the line ratios R as a function of $S2$ predicted by our models are compared with those of the observational sample. We can see that our photoionization models describe very well the region occupied by the observational data, indicating that the models are representative of real H II regions.

In order to eliminate any bias in our analysis that could be yielded by the extrapolation of our models out to the parameter space sampled by them, we only consider those objects listed in Table 1 whose estimated metallicities, ionization parameters and $T_{\rm eff}$ are in the ranges sampled by our grid of photoionization models: $0.03 \leqq Z/Z_\odot \leqq 1.0$, $-3.5 \leqq \log U \leqq -1.5$ and $30 \leqq T_{\rm eff}({\rm kK}) \leqq 40$. This make possible to estimate $T_{\rm eff}$ values for 865 ($\sim$72% of the sample) H II regions of our sample.

In Fig. 5, $Z/Z_\odot$ (lower panel) calculated using the Eq. 2 and $\log U$ (upper panel) calculated using the Eqs. 4, 5 and 6, as a function of the effective temperature $T_{\rm eff}$ for the 865 objects are presented. We can see that for most of the objects $T_{\rm eff}$ is higher than 36 kK, with an average value of $38.5(\pm 1.0)$ kK. Also in Fig. 5, the average and the standard deviation of these parameters considering different $T_{\rm eff}$ ranges (see Table 4) are shown. We can note that, despite the large dispersion, it seems that an anti-correlation be-
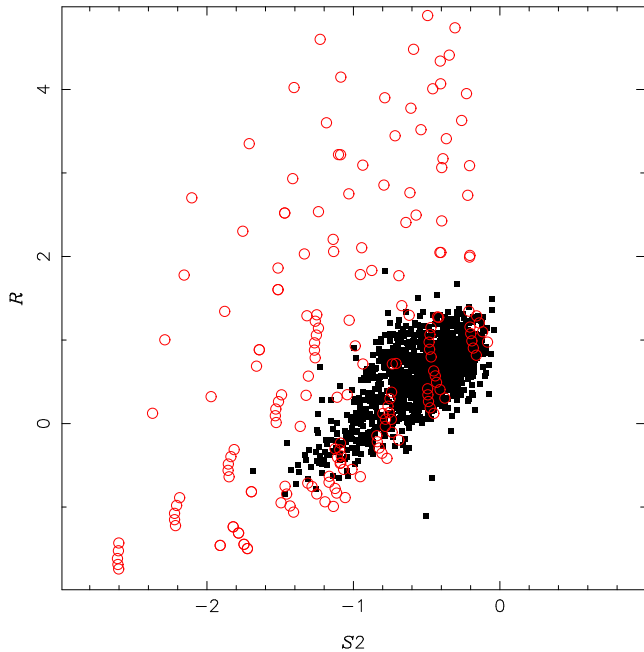
Figure 4. $R=\log([\text{O\,II}]\lambda\lambda3726+29/[\text{O\,III}]\lambda5007)$ vs. $S2=\log([\text{S\,II}](\lambda\lambda6717+31)/\text{H}\alpha)$. Black squares represent the observational data (see Sect. 3) while red circles the results of our models (see Sect. 2).

Figure 5. $Z/Z_\odot$ and $\log U$ as a function of T_{eff}. Points represents estimations for the sample presented in Table 1 for which were possible to compute the parameters considered. Error bars represent the standard deviation of the average values presented in Table 3. The error in T_{eff} was assumed to be 2 000 K (see Sect. 5).

Table 4. Average values of T_{eff}, $Z/Z_\odot$, and $\log(U)$, for the selected ranges of T_{eff}. The number of objects (N) used in these calculations are listed.

Range (10^3 K)	$< T_{\text{eff}} >$	$< Z/Z_\odot >$	$< \log U >$	N
30.0-32.5	—	—	—	0
32.5-35.0	34.28 ± 0.79	0.71 ± 0.18	-1.96 ± 0.40	3
35.0-37.5	36.84 ± 0.52	0.75 ± 0.14	-2.42 ± 0.24	140
37.5-40.0	38.85 ± 0.68	0.64 ± 0.23	-2.72 ± 0.35	722

Table 5. Coefficients of the linear regression $T_{\text{eff}}(\text{kK}) = a \times R(\text{kpc}) + b$ and the number of H II regions used for each galaxy.

Galaxy	a	b	Number
M 101	$+0.08(\pm0.02)$	$37.34(\pm0.32)$	21
NGC 300	$+0.33(\pm0.06)$	$37.86(\pm0.18)$	26
NGC 1512	$+0.13(\pm0.05)$	$36.58(\pm0.41)$	49
NGC 3621	$+0.11(\pm0.02)$	$37.29(\pm0.29)$	63
NGC 925	$+0.20(\pm0.04)$	$37.90(\pm0.21)$	16
NGC 2805	$+0.11(\pm0.02)$	$37.80(\pm0.34)$	12
UGC 9837	$+0.12(\pm0.05)$	$38.91(\pm0.25)$	29
NGC 1058	$+0.21(\pm0.07)$	$38.25(\pm2.54)$	91
NGC 1637	$0.00(\pm0.06)$	$38.75(\pm0.23)$	64
NGC 3310	$+0.04(\pm0.02)$	$39.24(\pm0.10)$	67
NGC 5474	$-0.26(\pm0.08)$	$40.08(\pm0.18)$	29
NGC 628	$+0.20(\pm0.04)$	$37.17(\pm0.25)$	125
NGC 1232	$+0.16(\pm0.02)$	$35.79(\pm0.31)$	16
NGC 3184	$0.00(\pm0.10)$	$37.53(\pm0.56)$	17

tween T_{eff} and $\log U$ is obtained. In contrast, no trend is found between T_{eff} and $Z/Z_\odot$.

In our sample there are 14 spiral galaxies for which there are emission lines measurements in least 10 H II regions distributed along their disks. Using these observations we estimate the T_{eff} of each H II region to investigate the behaviour of the T_{eff} as a function of the galactocentric distances R. In Table 5 the coefficients of the linear regressions are listed. These linear regressions together with the estimated T_{eff} for each H II region are plotted in Figs. 6 and 7 as a function of R (in kpc). For 11 galaxies we derive a positive slope, two objects (NGC 1647 and NGC 3184) present a null slope and only one galaxy (NGC 5474) shows a negative slope (see Table 5).

7   DISCUSSION

In the present work, we propose a calibration between the $R = \log([\text{O\,II}]\lambda\lambda3726+29/[\text{O\,III}]\lambda5007)$ index and T_{eff} based on photoionization models built assuming a match between the metalliciy of the gas phase of the hypothetical H II region and the one of the atmosphere of the ionizing stars.
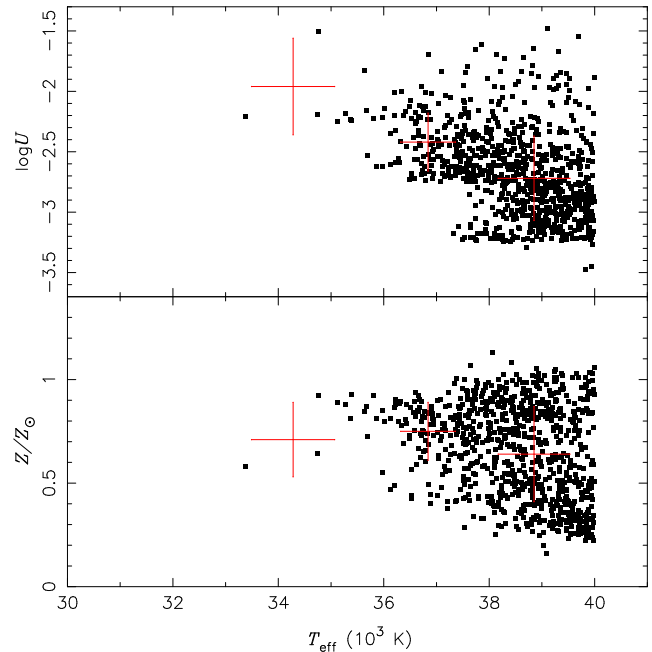
We took into account the dependence of the T_{eff}-R relation with the metallicity and with the ionizing parameter. Other emission-line ratios have also been proposed in the literature as T_{eff} indicators. For example, Kennicutt et al. (2000) used a grid of photoionization models and showed that the line ratios He I$\lambda5876$/Hβ, [O III]$\lambda5007$/Hβ, among others, can be used to estimate T_{eff}. Also, Oey et al. (2000) presented a detailed comparison of optical H II region spectra with photoionization models in order to investigate the reliability of some line ratios as T_{eff} indicators. These authors found that, among several line ratios considered, the [Ne III]$\lambda3869$/Hβ has higher sensitivity to T_{eff} and it is independent of morphology, and is insensitive to gas shocks, although it is abundance dependent.
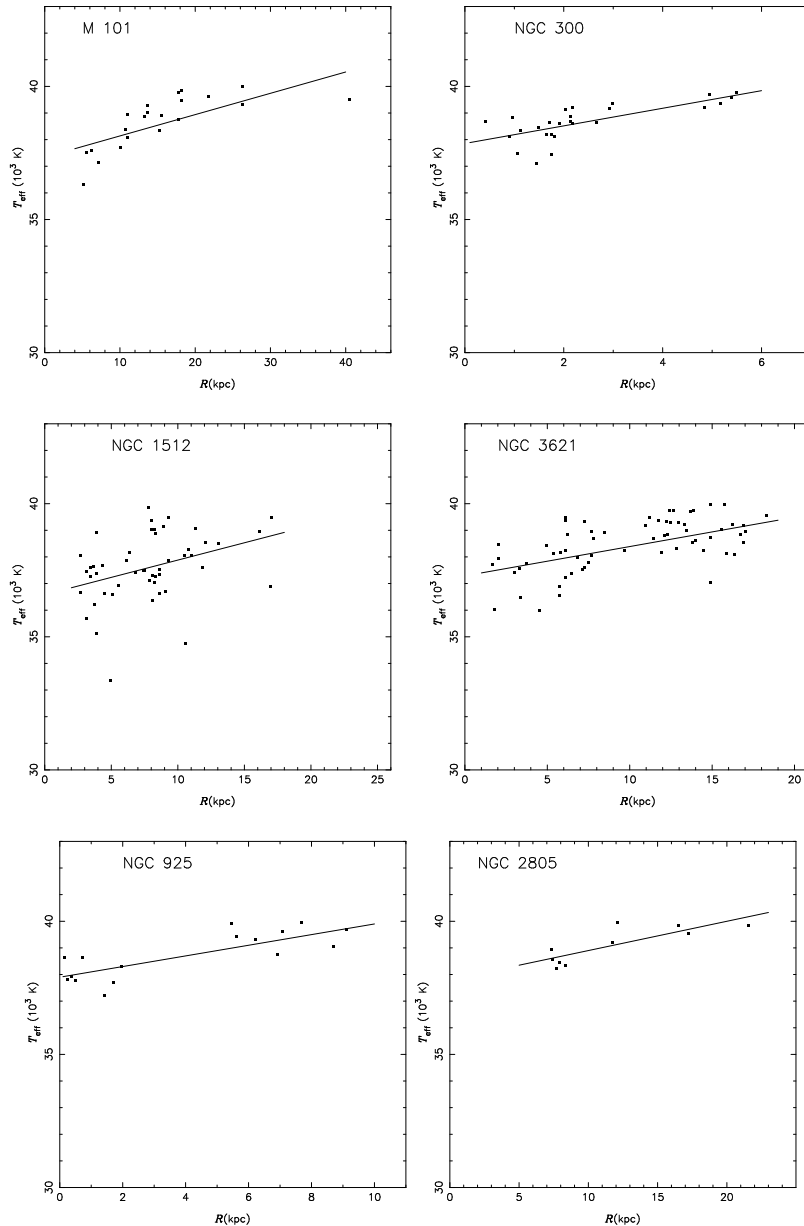
Figure 6. $T_{\rm eff}$ as a function of the galactocentric distance R for the indicated spiral galaxies. Solid lines represent the linear regressions whose coefficients are listed in Table 5. The assumed $T_{\rm eff}$ error was 1 500 K (see Sect. 5).

As in the case of the R index, $T_{\rm eff}$ estimations based on other emission-line ratios require the previous determination of the metallicity Z (or abundance) and of the ionization parameter U (Oey et al. 2000). In the present work, we propose that, to infer the $T_{\rm eff}$, the metallicity can be derived through a calibration based on the $T_{\rm e}$-method and U via a calibration between $S2$ and U which depends on Z. Finally $T_{\rm eff}$ is obtained from its relation with the R index.

To test the reliability of the results found in this work, we use the observational data of H II regions located in the Large Magellanic Cloud obtained by Zastrow et al. (2013) to estimate their $T_{\rm eff}$ by using the methodology presented in Sect. 4. The obtained $T_{\rm eff}$ were compared with those derived by Zastrow and collaborators, who built detailed pho-

toionization models in order to reproduce the emission line intensities of the individual objects in their sample.

In Table 6 we listed the $T_{\rm eff}$ estimations for the objects for which we were able to apply our methodology together with the $T_{\rm eff}$ values from Zastrow et al. (2013). The difference between both estimation are also listed. We considered the Zastrow et al. estimations obtained assuming the same atmosphere models used by us (WM-Basic models). We found that our $T_{\rm eff}$ values are systematically higher with an average difference of 1.45 kK, which is lower than our estimated uncertainties for the $T_{\rm eff}$ obtained through the R index (2.5 kK).

As can be seen in Fig. 5, where the $T_{\rm eff}$ estimations for part of our compiled sample (865 objects) are shown, we
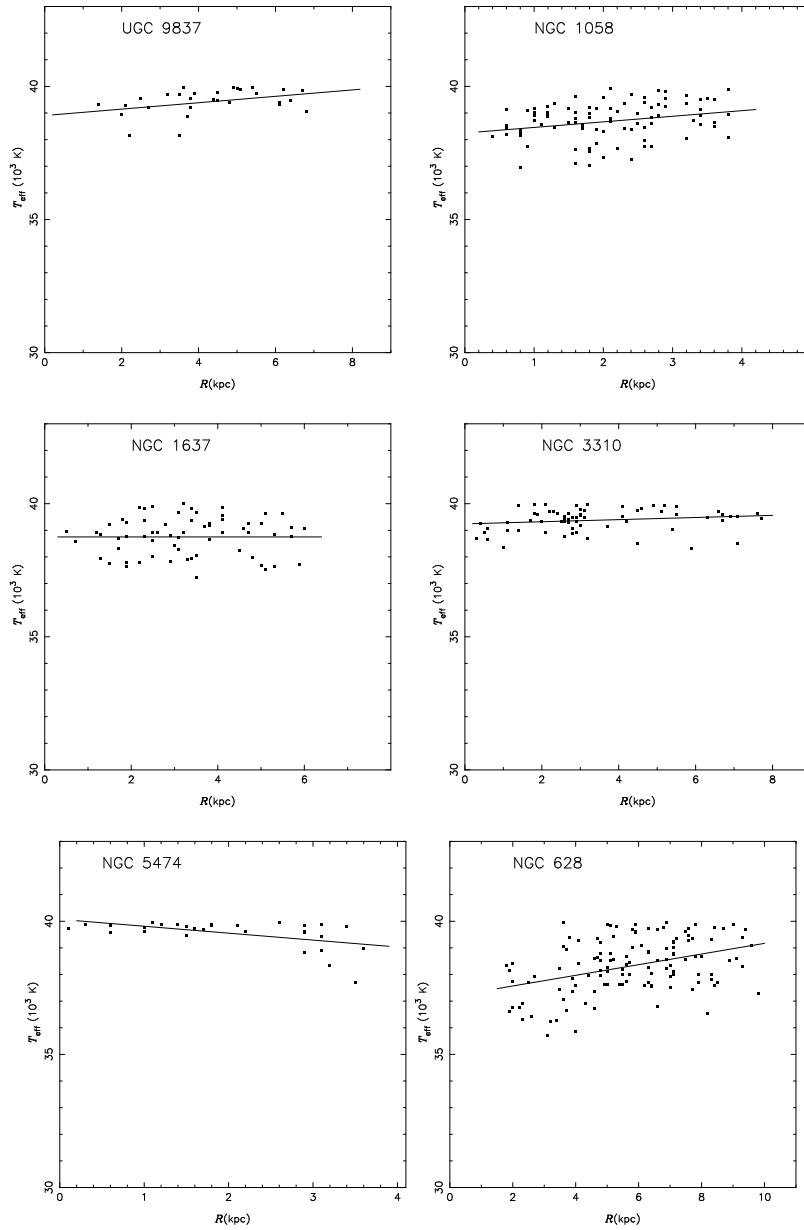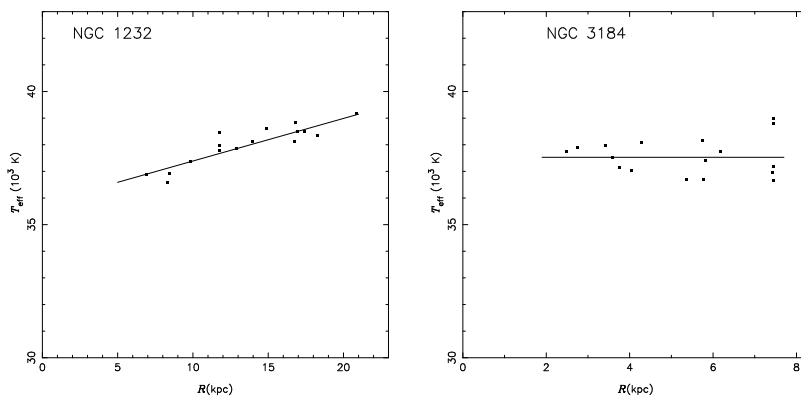
Figure 7. Same as Fig. 6.

Figure 8. Same as Fig. 6.

Table 6. $T_{\rm eff}$ values estimated from the R index and those from detailed photoionization models by Zastrow et al. (2013) for a sample of H II regions in the LMC.

Object	$T_{\rm eff}$ (kK)		Difference (kK)
	This paper	Zastrow et al.	
L 32	36.75	34.00	2.70
L 35	34.93	31.00	3.93
L 52	39.39	38.75	0.64
L 344	39.48	39.0	0.48
L 390	37.21	37.0	0.21
L 394	39.75	39.0	0.75

found that there is no correlation between $T_{\rm eff}$ and Z, at least for the $T_{\rm eff}$ values in the range of validity of the proposed $T_{\rm eff}$-R relationship ($30 \lesssim T_{\rm eff}({\rm kK}) \lesssim 40$). This result is in consonance with the one found by Morisset (2004), who comparing mid-infrared emission-line intensities of Galactic H II regions with photoionization model results did not find evidences of any correlation between $T_{\rm eff}$ and Z. Morisset (2004) showed that, not taking properly into account the effect of metallicity on the ionizing shape of the stellar atmosphere, would lead to an apparent decrease of $T_{\rm eff}$ with Z.

Regarding the $T_{\rm eff}$ variation along the disk of spiral galaxies, in a pioneer work, Shields & Searle (1976) interpreted that the enhancement of the equivalent width of the Hβ emission line of a sample of H II regions located in the spiral galaxy M 101, could be due to an increment of the temperature of the hottest exciting stars, implying higher $T_{\rm eff}$ of the radiation field. These authors also concluded that high metallicity H II regions have lower $T_{\rm eff}$ values than those with low metallicities. Other authors (Dors & Copetti 2003; Vílchez & Pagel 1988; Henry & Howard 1995; Dors & Copetti 2005) have derived similar results. This behaviour has been interpreted as being due to effects on the opacity of the stellar atmospheres rather than differences in the stellar masses (see Bresolin et al. 1999). In Figs. 6-8 we found positive $T_{\rm eff}$ gradients for 11 spiral galaxies, in agreement with the original idea by Shields & Searle (1976). Since our $T_{\rm eff}$-R relationship is only valid for $30{\rm kK} \lesssim T_{\rm eff} \lesssim 40{\rm kK}$, slopes of the $T_{\rm eff}$ gradients in spiral galaxies could be higher than the ones listed in Table 5. Dors & Copetti (2005) used photoionization models in order to reproduce the observed gradients of emission-line ratios for H II regions located in the normal spiral galaxy M 101 and in three barred spiral galaxies, namely NGC 1365, NGC 925, and NGC 1073. These authors derived positive $T_{\rm eff}$ gradients in the range 0.2-0.4 kK/kpc, with $T_{\rm eff}$ values up to 50 kK for the outermost regions of the disks of the galaxies analysed.

Fierro et al. (1986) compared observational emission-line intensities of H II regions located between 1 and 5 kpc from the centre of the spiral galaxy NGC 2403 with those predicted by a grid of photoionization models by Stasińska (1982). Fierro et al. (1986) found that models assuming $T_{\rm eff}=35\,{\rm kK}$ are able to reproduce the observational data (see also Evans 1986). Pérez-Montero & Vílchez (2009) used the $T_{\rm eff}$ sensitive parameter η' defined by pairs of consecutive ionization stages of the same species and introduced by Vílchez & Pagel 1988:

$$\eta' = \frac{I([{\rm O\,II}]\lambda\lambda3726 + 29\text{\AA})/I([{\rm O\,III}]\lambda\lambda4959 + 5007\text{\AA})}{(I([{\rm S\,II}]\lambda\lambda6717 + 31\text{\AA})/I([{\rm S\,III}]\lambda\lambda9069 + 9532\text{\AA})}.$$

They plotted this parameter as a function of the galactocentric distance for ten galaxies obtaining slopes ranging from 0.00 ± 0.01 to -0.11 ± 0.05. Taking into account that $T_{\rm eff}$ increases as η' decreases, this result is in agreement with our own. Nevertheless, the study of the $T_{\rm eff}$ behaviour along the disks of spiral galaxies still seems to be an open question in astronomy.

8 CONCLUSIONS

We have proposed a calibration for the effective temperatures of the radiation field of the ionizing star clusters of H II regions ($T_{\rm eff}$) as a function of the R=log([O II]$\lambda\lambda3726+29$/[O III]$\lambda5007$) index. This calibration is based on photoionization models assuming a match between the metallicity of both ionizing stars and the gas phase of the H II regions as well as considering the effect of the ionizing parameter on the R index. Since the R index shows small variations for $T_{\rm eff}$ values larger than 40 kK our method is valid in the range sampled by our models with metallicities ($Z/Z_\odot$) between 0.03 and 1, logarithm of the ionization parameter ($\log U$) between -3.5 and -1.5 and the effective temperature ($T_{\rm eff}$) between 30 and 40 kK. We found that this $T_{\rm eff}$-R relation has a strong dependence with the ionizing parameter while it shows a weak direct dependence with the metallicity (variations in Z translate into variations in U).

On the other hand taking advantage of that the [S II]($\lambda\lambda6717+31$)/Hα emission-line ratio is about constant for a large range of $T_{\rm eff}$, we calculated linear regressions between the ionization parameter and this line-ratio for the results of our models and for the different metallicity regimes considered. A large fraction of the variation of the ionization parameter is due to differences in the temperature of the ionizing stars through the amount of the hydrogen ionizing photons. Hence, the use of this particular line-ratio to derive the ionization parameter is preferable over others in the literature due to its (relatively) low dependence on the $T_{\rm eff}$.

In this work, we explored the different sources of uncertainties in the $T_{\rm eff}$ estimations finding that the main contribution comes from the probable multiple star presence as the ionizing source of the giant extragalactic H II regions rather than a single star. Small contributions comes from uncertainties in the ionization parameter and metallicity estimations, and from the emission-line measurements.

From the $T_{\rm eff}$ estimations for a sample of 865 H II regions, we did not find any correlation between $T_{\rm eff}$ and the metallicity. We found that most of the objects ($\sim$ 87%) present $T_{\rm eff}$ values in the range between 37 and 40 kK. Studying the $T_{\rm eff}$ gradients across the disks of 14 spiral galaxies through the use of the estimated $T_{\rm eff}$ of their H II regions we found that 11 of them have positive gradients, other 2 present flat gradients, and only one shows a negative gradient. Our results supports the original idea by Shields & Searle (1976) that there is a positive gradient of $T_{\rm eff}$ across the disks of spiral galaxies traced by H II regions although more work on this topic is required to confirm this

behaviour and to explain the presence of some flat and negative gradients.

REFERENCES

Allende-Prieto C., Lambert D. L., Asplund M., 2001, ApJ, 556, L63

Ambarzumian V. A., 1932, Nature, 129, 725

Baldwin J. A., Phillips M. M., Terlevich R. 1981, PASP, 93, 5

Berg D. A. et al., 2013, ApJ, 775, 128

Bosch G., Selman F., Melnick J., Terlevich R., 2001, A&A, 380, 13

Bresolin F., Kennicutt R. C., Garnett D. R., 1999, ApJ, 510, 104

Bresolin F., Garnett D. R., Kennicutt R. C., 2004, ApJ, 615, 228

Bresolin F. et al., 2009a, ApJ, 700, 309

Bresolin F., Kennicutt R. C., Ryan-Weber E., 2012, ApJ, 750, 122

Bresolin F., Ryan-Weber E., Kennicutt R. C., Goddard Q., 2009, ApJ, 695, 580

Bresolin F., Schaerer D., González Delgado R. M., Stasińska G., 2005, A&A, 441, 981

Caffau E. et al. 2016, A&A, 585, 16

Campbell A., 1988, ApJ, 335, 644

Cacho R., Sánchez-Blázquez P., Gorgas J., Pérez I., 2014, MNRAS, 442, 2496

Chopinet M., & Lortet-Zuckermann M. C., 1976, A&AS, 25, 179

Corti M., Bosch G., Niemela V., 2007, A&A, 467, 137

Copetti M. V. F., Castañeda H. O., Mallmann J. A. H., Schmidt A. A., 2000, A&A, 357, 621

Dors O. L., Krabbe A., Hägele G. F., Pérez-Montero E., 2011, MNRAS, 415, 3616

Dors O. L., & Copetti M. V. F., 2003, A&A, 404, 969

Dors O. L., & Copetti M. V. F., 2005, A&A, 437, 837

Dors O. L., Storchi-Bergmann T., Riffel R. A., Schimdt A. A. 2008, A&A, 482, 59

Dors O. L. et al., 2013, MNRAS, 432, 2512

Díaz A. I., Terlevich E., Castellanos M., Hägele G. F., 2007, MNRAS, 382, 251

Díaz A. I., Castellanos M., Terlevich E., Garícia-Vargas L. M., 2000, MNRAS, 318, 462

Díaz A. I., Terlevich E., Vílchez J. M., Pagel B. E. J., Edmunds M. G., 1991, MNRAS, 253, 245

de Koter A., Heap S. R., Hubeny I., ApJ, 477, 792

Evans C. J., Kennedy M. B., Dufton P. L., 2015, A&A, 574, 13

Evans I. N., 1986, ApJ, 309, 544

Evans I. N., & Dopita M. A., 1985, ApJS, 58, 125

Esteban C., & Méndez D. I., 1999, A&A, 348, 446

Fierro J., Torres-Peimbert S., Peimbert M., PASP, 1986, 98, 1032

Ferland G. J. et al., 2013, Rev. Mex. Astron. Astrofis., 49, 137

Garnett D. R., Shields G. A., Skillman E. D., Sagan S. P., Dufour R. J., 1997, ApJ, 489, 63

Garnett D. R., & Kennicutt R. C., 1994, ApJ, 426, 123

Gurzadyan G. A. 1955, Soob. Burakan Obs., 16, 3

Hägele, G. F., Díaz, Á. I., Terlevich, R., et al. 2013, MNRAS, 432, 810

Hägele G. F., Firpo V., Bosch G., Díaz A. I., Morrell N., 2012, MNRAS, 422, 3475

Hägele G. F. et al., 2011, MNRAS, 414, 272

Hägele, G. F., Díaz, Á. I., Cardaci, M. V., Terlevich, E., & Terlevich, R. 2010, MNRAS, 402, 1005

Hägele, G. F., Díaz, Á. I., Cardaci, M. V., Terlevich, E., & Terlevich, R. 2009, MNRAS, 396, 2295

Hägele G. F. et al., 2008, MNRAS, 383, 209

Hägele, G. F., Díaz, Á. I., Cardaci, M. V., Terlevich, E., & Terlevich, R. 2007, MNRAS, 378, 163

Hägele G. F., Pérez-Montero E., Díaz A. I., Terlevich E., Terlevich R., 2006, MNRAS, 372, 293

Henry R. B. C., & Howard J. W., 1995, ApJ, 438, 170

Hummer D. G., & Storey P. J., 1987, MNRAS, 224, 8018

Iijima T., 1981, in NATO Advanced Study Institute 69, Photom etric and Spectroscopic Binary Systems, 517

Kaler J. B., 1978, ApJ, 220, 887

Kaler J. B., 1976, ApJ, 210, 843

Köppen J., & Tarafdar S. P., 1978, A&A, 69, 363

Kennicutt D. R., Garnett D. R., 1996, ApJ, 456, 504

Kennicutt R. C., Bresolin F., Garnett D. R., 2003, ApJ, 591, 801

Kennicutt R. C., Bresolin F., French H., Martin P., 2000, ApJ, 537, 589

Kewley L. J., & Ellison S., 2008, ApJ, 681, 1183

Kewley L. J., & Dopita M. A., 2002, ApJS, 142, 35

Kewley L. J., Dopita M. A., Sutherland R. S., Heisler C. A., Trevena J., 2001, ApJ, 556, 121

Kwitter K. B., & Aller L. H., 1981, MNRAS, 195, 939

Krabbe A. C. et al., 2014, MNRAS, 437, 1155

Lamb J. B. et al., 2015, arXiv:1512.01233v1

Lee H., Skillman E. D., 2004, ApJ, 614, 698

Leitherer C. et al., 1999, ApJ, 123, 3

López-Sánchez A. R., Esteban C., García-Rojas J., Peimbert M., Rodríguez M., 2007, ApJ, 656, 168

López-Sánchez A. R., Mesa-Delgado A., López-Martn L., Esteban C., 2011, MNRAS, 411, 2076

López-Sánchez A. R., Esteban C., 2009, A&A, 508, 615

López-Hernández J. et al., 2013, MNRAS, 430, 472

Massey P., 2011, in Astronomical Society of the Pacific Conference Series, Vol. 440, UP2010: Have Observations Revealed a Variable Upper End of the Initial Mass Function ed. M. Treyer, T. Wyder, J. Neill, M. Seibert,& J. Lee, 29

Massey P., Zangari A. M., Morrell N. I., 2009, ApJ, 692, 618

Massey P. et al. 2005, ApJ, 627, 477

Mayya Y. D., & Prabhu T. P., 1996, AJ, 111, 1252

Morisset C., 2004, ApJ, 601, 858

Morisset C., 2016, arXiv160601146M

Morrell N. I., Massey P., Neugent K. F. 2014, ApJ, 789, 139

Mathis J. S., 1985, ApJ, 291, 247

Oey M. S., Dopita M. A., Shields J. C., Smith R. C. 2000, ApJSS, 128, 511

Osterbrock D. E., 1989, Astrophysics of Gaseous Nebulae and Active Galactic Nuclei. University Science Books, Mill Valley, CA

Pagel B. E. J., Edmunds M. G., Blackwell D. E., Chun M. S., Smith G., 1979, MNRAS, 189, 95

Pauldrach A. W. A., Hoffmann T. L., Lennon M., 2001, A&A, 375, 161

Pellegrini E. W., Baldwin J. A., Ferland G. J., 2011, ApJ, 738, 34

Pellegrini E. W., Baldwin J. A., Ferland G. J., 2010, ApJSS, 191, 160

Peña-Guerrero M. A., Peimbert A., Peimbert M., 2012, ApJ, 756, 14

Pérez-Montero E., 2014, MNRAS, 441, 2663

Pérez-Montero E., & Vílchez J. M., 2009, MNRAS, 400, 1721

Pérez-Montero E., & Contini T., 2009, MNRAS, 398, 949

Pérez-Montero E., & Díaz A. I. 2006, MNRAS, 449, 193

Pettini M., & Pagel B. E. J., 2004, MNRAS, 348, 59

Pilyugin L. S., Grebel E. K., Mattsson L., 2012, MNRAS, 424, 2316

Pilyugin L. S., & Grebel E. K., 2016, MNRAS, 457, 3678

Pilyugin L. S., 2001, A&A, 369, 594

Pilyugin L. S., 2000, A&A, 362, 325

reite-Martinez A., & Pottasch S. R., 1983, A&A, 126, 31

Rosa D. A. et al., 2014, MNRAS, 444, 2005

Russel S. S., & Dopita M. A., 1990, ApJS, 74, 93

Sanders R. L. et al., 2016, ApJ, 816, 23

Sánchez S. F. et al., 2012, A&A, 546, 2

Schaerer D., & de Koter A., 1997, A&A, 322, 598

Shields G. A., & Searle L., 1978, ApJ, 222, 821

Skillman E. D., & Kennicutt R. C., 1993, ApJ, 411, 655

Salpeter E. E., 1955, ApJ, 121, 161

Sota A., Maíz Apellániz J., Morrell N. I. et al., 2014, ApJS, 211, 10

Sota A., Maíz Apellániz J., Walborn N. R., 2011, ApJS, 193, 24

Stasinska G., & Tylenda R., 1986, A&A, 155, 137

Stasinska G., 1982, A&ASS, 84, 320

Storey P. J., & Zeipper C. J., 2000, MNRAS, 312, 813

Stoy R. H., 1933, MNRAS, 93, 588

Vacca W. D., Garmany C. D., Shull J. M., 1996, ApJ, 460, 914

van Hoof, P. A. M., Weingartner, J. C., Martin, P. G., Volk, K., & Ferland, G. J. 2001, in Challenges of Photoionized Plasmas, ed. G. Ferland & D. Savin (San Francisco: ASP), ASP Conf Ser., 247, 363

van Zee L., 2000, ApJ, 543, L31

van Zee L., Salzer J. J., Haynes M. P., O'Donoghue A. A., Balonek T. J., 1998, AJ, 116, 2805

Veilleux S., Osterbrock D. E. 1987, ApJS, 63, 295

Vermeij R., Damour F., van der Hulst J. M., Baluteau J.-.P, 2002, A&A, 390, 649

Vila-Costas, M. B., & Edmunds, M. G. 1993, MNRAS, 265, 199

Vílchez J. M., & Pagel B. E. J., 1988, MNRAS, 231, 257

Vílchez J. M., Pagel B. E. J., Díaz A. I., Terlevich E., Edmunds M. G., 1988, MNRAS, 235, 633

Zanstra, H. 1931, Publ. Dominion Astrophys. Obs., 4, 209

Zastrow, J., Oey M. S., Pellegrini E. W., 2013, ApJ, 769, 94

Zurita A., & Bresolin F., 2012, MNRAS, 427, 1463

Walborn N. R., Sana H., Simón-Díaz S., 2014, A&A, 564, 40